Models for Conjugated Metal Acetylide Polymers: Ruthenium Oligothienylacetylide Complexes

Yongbao Zhu, Dylan B. Millet, Michael O. Wolf,* and Steven J. Rettig†

Department of Chemistry, The University of British Columbia, Vancouver, British Columbia, Canada V6T 1Z1

Received August 7, 1998

The series of ruthenium(II) mono(oligothienylacetylide) complexes *trans*-Ru(dppm)$_2$(Cl)-(C≡CR) (dppm = $Ph_2PCH_2PPh_2$; R = 2-thienyl (**1a**), 5-(2,2′-bithienyl) (**1b**), and 5-(2,2′:5′,2″-terthienyl) (**1c**)) and bis(oligothienylacetylide) complexes *trans*-Ru(dppm)$_2$(C≡CR)$_2$ (R = 2-thienyl (**2a**), 5-(2,2′-bithienyl) (**2b**), and 5-(2,2′:5′,2″-terthienyl) (**2c**)) were synthesized. Complex **2c** was crystallographically characterized. The cyclic voltammograms of complexes **1a**−**c** all contain two oxidation waves, a Ru(II/III) wave and a ligand-based oxidation wave. As the length of the conjugated oligothienyl ligand increases, the thiophene-based oxidation wave becomes more chemically reversible. Complexes **2a**−**c** all have a Ru(II/III) wave in their cyclic voltammograms, as well as multiple ligand-based oxidation waves. Complexes **2b** and **2c** both form films on the electrode surfaces upon repeated cycling in the range 0−1.4 V vs SCE. The UV−vis spectra of complexes **1a**−**c** and **2a**−**c** all contain intense absorptions due to the $\pi-\pi^*$ transition in the oligothienyl ligand, and these appear at lower energy than the $\pi-\pi^*$ transitions in the corresponding oligothiophenes. The monocations **1c**$^+$ and **2c**$^+$ were synthesized in solution at −20 °C and were characterized by visible and near-IR spectroscopy. The $\pi-\pi^*$ transitions of the terthienyl ligand in **1c**$^+$ and **2c**$^+$ shift to higher energy compared with the analogous transitions in **1c** and **2c**, and a series of LMCT absorption bands of high intensity appear between 500 and 700 nm and between 900 and 1700 nm, respectively. These results support the conclusion that the π system of the conjugated oligothienyl ligands interacts strongly with the Ru(III) center.

Introduction

Metal acetylide polymers are of significant current interest because of their potential applications as low-dimensional conductors[1] and nonlinear optical materials.[2−6] Although many metal acetylide polymers have been prepared,[7−34] few have significant conductivities. A metal acetylide polymer can conduct only if charge can be delocalized along the entire polymer backbone, including the organic and metal fragments. Frapper and Kertesz have predicted, using extended Hückel theory,

* To whom correspondence should be addressed. E-mail: mwolf@chem.ubc.ca. Fax: 604-822-2847.

† Professional Officer: UBC Structural Chemistry Laboratory.

(1) Torrance, J. B. In *Low Dimensional Conductors and Superconductors*; Jerome, D., Caron, L. G., Eds.; NATO ASI Series 155; Plenum: New York, 1987; p 155.

(2) *Materials for Nonlinear Optics: Chemical Perspectives*; Stucky, G. D., Marder, S. R., Sohn, J., Eds.; American Chemical Society: Washington, DC, 1991.

(3) Whittall, I. R.; Humphrey, M. G.; Houbrechts, S.; Maes, J.; Persoons, A.; Schmid, S.; Hockless, D. C. R. *J. Organomet. Chem.* **1997**, *544*, 277−283.

(4) Whittall, I. R.; Cifuentes, M. P.; Humphrey, M. G.; Lutherdavies, B.; Samoc, M.; Houbrechts, S.; Persoons, A.; Heath, G. A.; Hockless, D. C. R. *J. Organomet. Chem.* **1997**, *549*, 127−137.

(5) McDonagh, A. M.; Whittall, I. R.; Humphrey, M. G.; Hockless, D. C. R.; Skelton, B. W.; White, A. H. *J. Organomet. Chem.* **1996**, *523*, 33−40.

(6) McDonagh, A. M.; Cifuentes, M. P.; Whittall, I. R.; Humphrey, M. G.; Samoc, M.; Lutherdavies, B.; Hockless, D. C. R. *J. Organomet. Chem.* **1996**, *526*, 99−103.

(7) Porter, P. L.; Guha, S.; Kang, K.; Frazier, C. C. *Polymer* **1991**, *32*, 1756−1760.

(8) Johnson, B. F. G.; Kakkar, A. K.; Khan, M. S.; Lewis, J. *J. Organomet. Chem.* **1991**, *409*, C12−C14.

(9) Sun, Y.; Taylor, N. J.; Carty, A. J. *Organometallics* **1992**, *11*, 4293−4300.

(10) Chawdhury, N.; Köhler, A.; Friend, R. H.; Younus, M.; Long, N. J.; Raithby, P. R.; Lewis, J. *Macromolecules* **1998**, *31*, 722−727.

(11) Irwin, M. J.; Vittal, J. J.; Puddephatt, R. J. *Organometallics* **1997**, *16*, 3541−3547.

(12) Sonogashira, K.; Takahashi, S.; Hagihara, N. *Macromolecules* **1977**, *10*, 879−880.

(13) Sonogashira, K.; Kataoka, S.; Takahashi, S.; Hagihara, N. *J. Organomet. Chem.* **1978**, *160*, 319−327.

(14) Davies, S. J.; Johnson, B. F. G.; Lewis, J.; Raithby, P. R. *J. Organomet. Chem.* **1991**, *414*, C51−C53.

(15) Khan, M. S.; Davies, S. J.; Kakkar, A. K.; Schwartz, D.; Lin, B.; Johnson, B. F. G.; Lewis, J. *J. Organomet. Chem.* **1992**, *424*, 87−97.

(16) Khan, M. S.; Pasha, N. A.; Kakkar, A. K.; Raithby, P. R.; Lewis, J.; Fuhrmann, K.; Friend, R. H. *J. Mater. Chem.* **1992**, *2*, 759−760.

(17) Khan, M. S.; Schwartz, D. J.; Pasha, N. A.; Kakkar, A. K.; Lin, B.; Raithby, P. R.; Lewis, J. *Z. Anorg. Allg. Chem.* **1992**, *616*, 121−124.

(18) Khan, M. S.; Kakkar, A. K.; Long, N. J.; Lewis, J.; Raithby, P.; Nguyen, P.; Marder, T. B.; Wittmann, F.; Friend, R. H. *J. Mater. Chem.* **1994**, *4*, 1227−1232.

(19) Johnson, B. F. G.; Kakkar, A. K.; Khan, M. S.; Lewis, J.; Dray, A. E.; Friend, R. H.; Wittmann, F. *J. Mater. Chem.* **1991**, *1*, 485−486.

(20) Lewis, J.; Khan, M. S.; Kakkar, A. K.; Johnson, B. F. G.; Marder, T. B.; Fyfe, H. B.; Wittmann, F.; Friend, R. H.; Dray, A. E. *J. Organomet. Chem.* **1992**, *425*, 165−176.

(21) Russo, M. V.; Furlani, A.; Altamura, P.; Fratoddi, I.; Polzonetti, G. *Polymer* **1997**, *38*, 3677−3690.

(22) Abe, A.; Kimura, N.; Tabata, S. *Macromolecules* **1991**, *24*, 6238−6243.

(23) Fyfe, H. B.; Mlekuz, M.; Zargarian, D.; Taylor, N. J.; Marder, T. B. *J. Chem. Soc., Chem. Commun.* **1991**, 188−190.

(24) Hagihara, N.; Sonogashira, K.; Takahashi, S. *Adv. Polym. Sci.* **1981**, *41*, 149−179.

(25) Markwell, R. D.; Butler, I. S.; Kakkar, A. K.; Khan, M. S.; Al-Zakwani, Z. H.; Lewis, J. *Organometallics* **1996**, *15*, 2331−2337.

(26) Dray, A. E.; Wittmann, F.; Friend, R. H.; Donald, A. M.; Khan, M. S.; Lewis, J.; Johnson, B. F. G. *Synth. Met.* **1991**, *41*−*43*, 871−874.

10.1021/om980677j CCC: $18.00
Publication on Web 04/20/1999

that conductivity in this class of materials should be possible, given the appropriate choice of metal and coordination environment.[35]

We and others have previously examined the electronic interactions between two terminal ferrocenyl groups bridged by a ruthenium bis(acetylide) group.[36−38] These studies have shown that the ruthenium bis(acetylide) bridge allows delocalization of charge between the two ferrocenyl groups and that the delocalization varies with the nature of the ancillary ligands surrounding the ruthenium. These results suggest that linking ruthenium bis(acetylide) bridges with conjugated organic moieties could result in electronic conductivity in such materials. Lewis and co-workers have synthesized ruthenium bis(acetylide) polymers where the metals are linked by phenyl bridges;[27,28] however, no electronic properties have been reported to date for these materials. Although phenyl bridges are readily accessible synthetically, it may be necessary to link the metal centers in these polymers with organic fragments which are more electron-rich and have longer conjugation lengths in order to enhance delocalization of charge.

Organic conducting polymers such as polythiophene have been extensively investigated for their remarkable electronic properties,[39] and it has been demonstrated that block copolymers containing short oligomers (four thiophene units) are sufficient for conductivity to be observed.[39,40] This suggests that metal acetylide polymers containing oligothienyl bridges may be good candidates for conducting materials. Toward this end, Raithby and co-workers have prepared dimeric platinum acetylide complexes containing oligothienyl bridges and demonstrated that the presence of the Pt centers in these complexes serves to lower the energy of the $\pi-\pi^*$ transition.[41] Bimetallic complexes of Fe, Ru, and Os containing conjugated bridges have also been recently shown to exhibit significant metal−metal interaction.[42]

Scheme 1

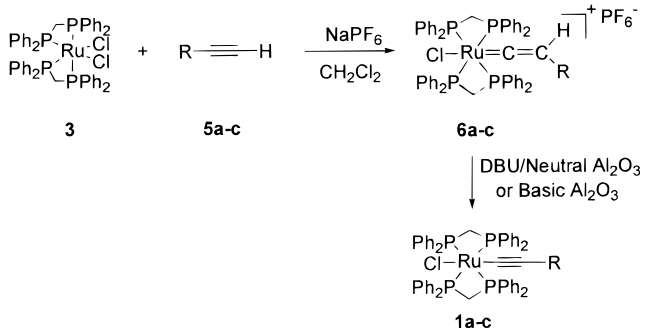

Scheme 2

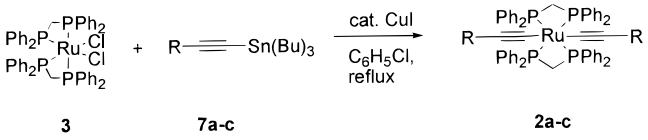

In this study, the 2,5-thiophenediyl bridge was found to permit the greatest degree of electronic interaction between metals among the conjugated bridges examined.

In a metal-containing conducting polymer, it is critical that the overlap between the metal dπ orbitals and the π system of the oligothiophene bridge permit charge delocalization. In this study, we have prepared ruthenium(II) mono(oligothienylacetylide) complexes **1a**−**c** and bis(oligothienylacetylide) complexes **2a**−**c**, to probe the interactions between the metal moiety and the organic fragment.

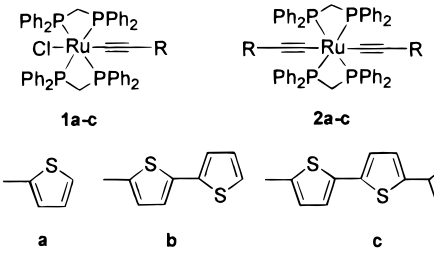

Results

Syntheses. Complexes **1a**−**c** were synthesized by coupling *cis*-Ru(dppm)$_2$Cl$_2$ (**3**) with oligothienylacetylenes **5a**−**c** in the presence of excess $NaPF_6$, yielding ruthenium vinylidene complexes **6a**−**c** (Scheme 1). Complexes **6a**−**c** were converted to **1a**−**c** either by passing them through a basic Al_2O_3 column or by reacting them with 1,8-diazabicyclo[5.4.0]undec-7-ene (DBU).

Bis(acetylide) complexes **2a**−**c** were prepared via the coupling of **3** with the corresponding 1-(tributylstannyl)-2-(oligothienyl)acetylenes **7a**−**c** in the presence of catalytic CuI (Scheme 2). The reactions were carried out in the absence of light in chlorobenzene heated to reflux. Complexes **1a**−**c** and **2a**−**c** were fully characterized using ^{1}H and ^{31}P NMR, IR, and UV−vis spectroscopy, and the elemental analyses were in the expected range. In solution, all the complexes decompose slowly when exposed to ambient light.

The ^{1}H NMR spectrum of **1c** shows broadened peaks assigned to the protons close to the ruthenium, and a

(27) Atherton, Z.; Faulkner, C. W.; Ingham, S. L.; Kakkar, A. K.; Khan, M. S.; Lewis, J.; Long, N. J.; Raithby, P. R. *J. Organomet. Chem.* **1993**, *462*, 265−270.
(28) Faulkner, C. W.; Ingham, S. L.; Khan, M. S.; Lewis, J.; Long, N. J.; Raithby, P. R. *J. Organomet. Chem.* **1994**, *482*, 139−145.
(29) Marder, T. B.; Lesley, G.; Yuan, Z.; Fyfe, H. B.; Chow, P.; Stringer, G.; Jobe, I. R.; Taylor, N. J.; Williams, I. D.; Kurtz, S. K. *ACS Symp. Ser.* **1991**, *No. 455*, 606−615.
(30) Takahashi, S.; Kariya, M.; Yatake, T.; Sonogashira, K.; Hagihara, N. *Macromolecules* **1978**, *11*, 1063−1066.
(31) Takahashi, S.; Murata, E.; Sonogashira, K.; Hagihara, N. *J. Polym. Sci., Polym. Chem. Ed.* **1980**, *18*, 661−669.
(32) Takahashi, S.; Ohyama, Y.; Murata, E.; Sonogashira, K.; Hagihara, N. *J. Polym. Sci., Polym. Chem. Ed.* **1980**, *18*, 349−353.
(33) Takahashi, S.; Morimoto, H.; Murata, E.; Kataoka, S.; Sonogashira, K.; Hagihara, N. *J. Polym. Sci., Polym. Chem. Ed.* **1982**, *20*, 565−573.
(34) Kotani, S.; Shiina, K.; Sonogashira, K. *Appl. Organomet. Chem.* **1991**, *5*, 417−425.
(35) Frapper, G.; Kertesz, M. *Inorg. Chem.* **1993**, *32*, 732−740.
(36) Colbert, M. C. B.; Lewis, J.; Long, N. J.; Raithby, P. R.; White, A. J. P.; Williams, D. J. *J. Chem. Soc., Dalton Trans.* **1997**, 99−104.
(37) Jones, N. D.; Wolf, M. O.; Giaquinta, D. M. *Organometallics* **1997**, *16*, 1352−1354.
(38) Zhu, Y.; Clot, O.; Wolf, M. O.; Yap, G. P. A. *J. Am. Chem. Soc.* **1998**, *120*, 1812−1821.
(39) *Handbook of Conducting Polymers*; Skotheim, T. A., Ed.; Marcel Dekker: New York, 1986.
(40) Hong, Y.; Miller, L. L. *Chem. Mater.* **1995**, *7*, 1999−2000.
(41) Lewis, J.; Long, N. J.; Raithby, P. R.; Shields, G. P.; Wong, W.-Y.; Younus, M. *J. Chem. Soc., Dalton Trans.* **1997**, 4283−4288.
(42) Colbert, M. C. B.; Lewis, J.; Long, N. J.; Raithby, P. R.; Younus, M.; White, A. J. P.; Williams, D. J.; Payne, N. N.; Yellowlees, L.; Beljonne, D.; Chawdhury, N.; Friend, R. H. *Organometallics* **1998**, *17*, 3034−3043.

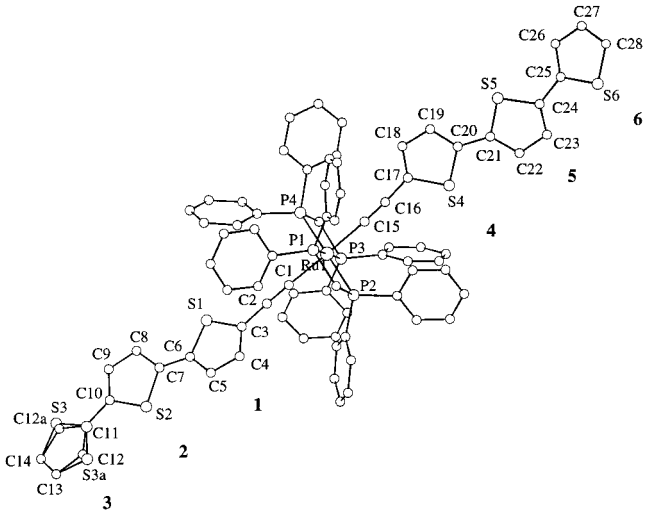

Figure 1. X-ray crystal structure of **2c**.

Table 1. Selected Bond Lengths (Å) and Angles (deg) for 2c

Ru(1)−P(1)	2.3306(8)	Ru(1)−C(1)	2.059(3)
Ru(1)−P(2)	2.3298(7)	Ru(1)- C(15)	2.067(3)
Ru(1)−P(3)	2.3243(8)	C(1)−C(2)	1.195(4)
Ru(1)−P(4)	2.3340(7)	C(15)−C(16)	1.200(4)
P(1)−Ru(1)−P(2)	72.65(3)	P(3)−Ru(1)−C(1)	92.09(8)
P(1)−Ru(1)−P(3)	178.63(3)	P(3)−Ru(1)−C(15)	90.92(9)
P(1)−Ru(1)−P(4)	108.70(3)	P(4)−Ru(1)−C(1)	92.20(7)
P(2)−Ru(1)−P(3)	106.12(3)	P(4)−Ru(1)−C(15)	88.38(7)
P(2)−Ru(1)−P(4)	178.42(3)	C(1)−Ru(1)−C(15)	176.97(12)
P(3)−Ru(1)−P(4)	72.52(3)	Ru(1)−C(1)−C(2)	176.4(3)
P(1)−Ru(1)−C(1)	87.26(8)	Ru(1)−C(15)−C(16)	175.5(3)
P(1)−Ru(1)−C(15)	89.74(9)	C(1)−C(2)−C(3)	177.2(3)
P(2)−Ru(1)−C(1)	87.03(7)	C(15)−C(16)−C(17)	174.8(4)
P(2)−Ru(1)−C(15)	92.46(7)		

single broadened peak was observed in the ^{31}P NMR spectrum. The broadened peaks sharpened when diisopropylamine was added to the NMR solution, and no new resonances were observed in the ^{31}P NMR spectrum, consistent with the broadening being a result of partial oxidation to the paramagnetic Ru(III) species and in situ reduction with diisopropylamine. It is possible that **1c** oxidizes slowly in solution when exposed to air or that a trace amount of the Ru(III) species is formed on the basic alumina in the last step of the synthesis; however, this is the only compound in the series for which any peak broadening was consistently observed in the NMR spectra.

Complex **2c** was crystallized from layered methylene chloride−hexanes at 4 °C to give orange irregular crystals whose structure was determined by single-crystal X-ray diffraction (Figure 1). Selected bond lengths and angles are listed in Table 1. The ruthenium center is in a distorted-octahedral environment with the two terthienylacetylide ligands in a trans orientation around the Ru. The dihedral angles between the six thiophene rings in the structure are of interest, since the extent of conjugation depends on the coplanarity of the rings. The thiophene rings have been labeled 1−6 in Figure 1. The dihedral angle between the two innermost thiophene rings (1 and 4) is 47.2°. The dihedral angles between rings 1−2 and 4−5 are small, 9.3 and 2.6° respectively, indicating that these rings are held nearly coplanar in the solid-state structure. Both terminal thiophene rings (3 and 6) are disordered with respect to 180° rotation about the bond to the adjacent ring and have dihedral angles with the adjacent rings of 17.8° (2−3) and 27.6° (5−6).

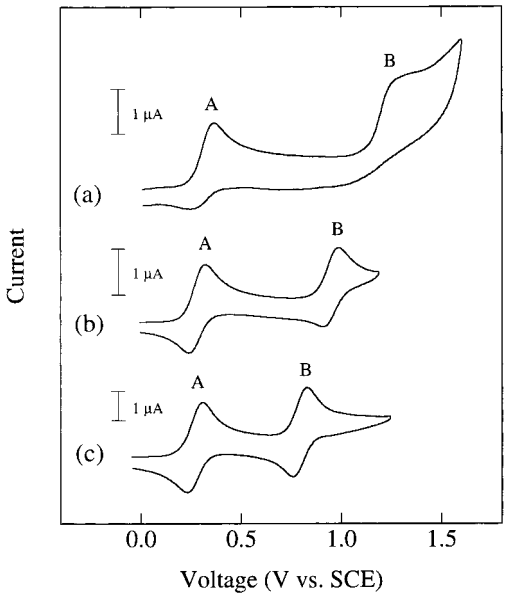

Figure 2. Cyclic voltammograms of (a) **1a** (2.2×10^{-3} M), (b) **1b** (1.6×10^{-3} M), and (c) **1c** (1.8×10^{-3} M) in CH_2Cl_2 containing 0.1 M $[(n\text{-}Bu)_4N]PF_6$. The scan rate was 100 mV/s.

Cyclic Voltammetry. Complexes **1a**−**c** all have two oxidation waves in their cyclic voltammograms (Figure 2) in the range 0.0−1.6 V vs SCE. Wave A was assigned to the Ru(II/III) oxidation, since it appears at similar potentials in all three complexes (Table 2). The related complexes *trans*-Ru(dppm)$_2$(Cl)(C≡CR′) (R′ = phenyl, 4-nitrophenyl) have oxidation waves due to the Ru(II/III) process with $E_p = 0.41$ V vs SCE for R′ = phenyl and 0.59 V vs SCE for R′ = 4-nitrophenyl.[43] Inspection of the first oxidation waves (A) for **1a**−**c** reveals features diagnostic of chemical irreversibility. For all these complexes plots of $i_{p,a}$ vs $v^{1/2}$ deviate from linearity, and the ratio $i_{p,c}/i_{p,a}$ is less than 1 (Table 2), consistent with some of the oxidized species undergoing following chemical reactions.[44] These results suggest that isolation of the Ru(III) complexes may be difficult, due to the instability of the oxidized species in solution. The $i_{p,c}/i_{p,a}$ ratio for **1c** is closest to 1; therefore, we assume that the oxidized form of this complex is most likely to be sufficiently stable to isolate. Attempts to isolate the Ru(III) complex by oxidation of **1c** using ferrocenium hexafluorophosphate yielded a deeply colored gray-green solid; however, this complex was found to be impure. The IR spectrum of this solid contains an unassigned band at 1920 cm^{-1} in addition to the expected peak at 1976 cm^{-1}.[45] In addition, electrochemical reduction of the oxidized **1c** yielded other products in addition to **1c**, as indicated by new resonances in the ^{31}P NMR spectrum. Although all attempts to isolate the Ru(III)

(43) These complexes have been prepared previously but were not characterized by cyclic voltammetry. See: Hodge, A. J.; Ingham, S. L.; Kakkar, A. K.; Khan, M. S.; Lewis, J.; Long, N. J.; Parker, D. G.; Raithby, P. R. *J. Organomet. Chem.* **1995**, *488*, 205−210.

(44) Brown, E. R.; Sandifer, J. In *Physical Methods of Chemistry*; Rossiter, B. W., Hamilton, J. F., Eds.; Wiley: New York, 1986; Vol. 2.

(45) Sato, M.; Shintate, H.; Kawata, Y.; Sekino, M.; Katada, M.; Kawata, S. *Organometallics* **1994**, *13*, 1956−1962.

Table 2. IR, UV−Vis−Near-IR, and Cyclic Voltammetry Data

complex	UV−vis−near-IR λ (nm) ($\epsilon \times 10^{-3}$ (M^{-1} cm^{-1}))[a]	IR (KBr) $\nu_{C\equiv C}$ (cm^{-1})	E_p(Ru(II/III) (V vs SCE)[b]	$i_{p,c}/i_{p,a}$[b,c]	E_p(second wave) (V vs SCE)[b]
1a	328 (14)	2063	0.36	0.50	1.25
1b	406 (22)	2056	0.32	0.89	0.99
1c	334 (sh) (11), 450 (33)	2053	0.30	0.94	0.84
1c$^+$	375 (13), 580 (29), 665 (sh) (17), 1090 (29)				
2a	338 (25)	2050	0.33	0.59	0.98
2b	420 (53)	2050	0.30	0.95	0.85
2c	340 (sh) (24), 460 (75)	2047	0.30	0.95	0.76
2c$^+$	400 (45), 595 (28), 1330 (23), 1610 (sh) (16)				
4c	384 (34)	2139			1.07[d]

[a] Conditions: CH_2Cl_2, 20 °C; except for **1c**$^+$ and **2c**$^+$, which were obtained at −17 °C. sh = shoulder. [b] Conditions: Pt working electrode; 20 °C; CH_2Cl_2; scan rate 100 mV/s. [c] Ru(II/III) wave. [d] First oxidation wave.

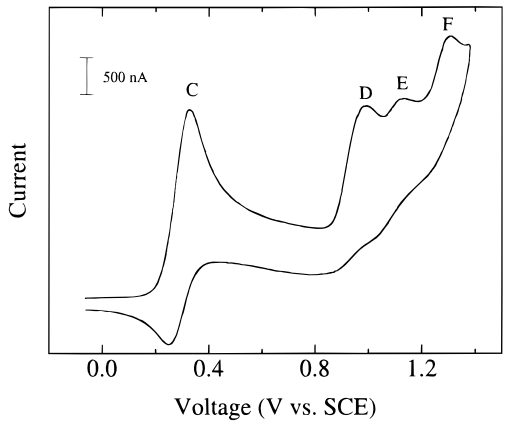

Figure 3. Cyclic voltammogram of **2a** in CH_2Cl_2 containing 0.1 M [(*n*-Bu)$_4$N]PF_6. The scan rate was 100 mV/s.

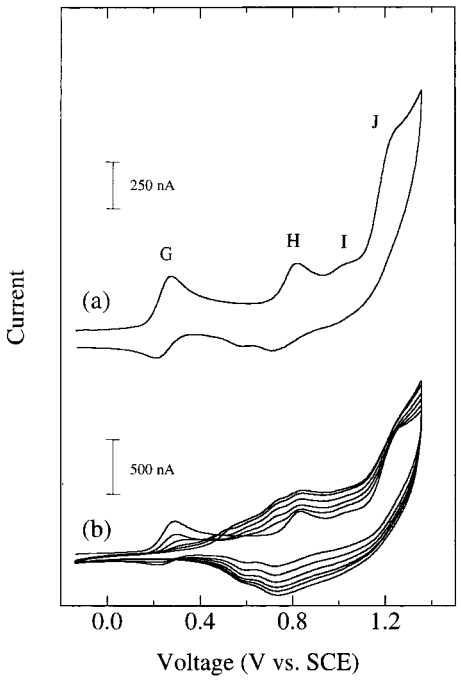

Figure 4. (a) Single-scan cyclic voltammogram of **2b** (4.0×10^{-4} M) in CH_2Cl_2 containing 0.1 M [(*n*-Bu)$_4$N]PF_6. (b) Multiple-scan cyclic voltammogram of **2b** (4.0×10^{-4} M). The scan rate was 100 mV/s.

complex as a pure solid were unsuccessful, we were able to spectroscopically characterize this species in situ (vide infra).

The second oxidation wave (B) in the cyclic voltammogram of **1a** is clearly chemically irreversible. For complex **1b**, wave B becomes more reversible only at high scan rates (≥100 mV/s) but is irreversible at slower scan rates. Wave B appears most chemically reversible for **1c**. The oxidation potential of wave B decreases significantly as the length of the oligothienyl ligand increases (Table 2). On the basis of this behavior, the second oxidation wave (B) is assigned to a thiophene-based oxidation. Electrochemical studies on oligothiophenes have shown that longer oligomers have lower oxidation potentials.[46] The potential of wave B in **1c** is lower and more reversible than the first oxidation wave in the cyclic voltammogram of the organic oligomer **4c** (E_p = 1.07 V vs SCE). At the potential of wave B the ruthenium in **1c** is already oxidized yet is still able to stabilize the ligand-based oxidation relative to the trimethylsilyl derivative **4c**.

The cyclic voltammograms of complexes **2a**−**c** all contain multiple waves. Complexes **2a** and **2b** both show four distinct waves in the range 0−1.4 V vs SCE (Figures 3 and 4a). The lowest potential waves (C for **2a**; G for **2b**) are assigned to the Ru(II/III) redox couple. Wave G is more reversible than wave C, as shown by $i_{p,c}/i_{p,a}$ measurements, and wave C becomes more reversible at higher scan rates. The three irreversible waves (D−F for **2a**; H−J for **2b**) observed at higher potentials are assigned to ligand-based oxidations, as well as oxidation of products resulting from decomposition during the electrochemical experiment. It is very clear that the first of these multiple waves (D and H) are ligand-based and are likely due to the same process which gives rise to wave B in the cyclic voltammograms of **1a**−**c**.

For complex **2b** repeated scans over the range 0−1.4 V result in an increase in the current upon each subsequent scan (Figure 4b), consistent with deposition of conducting material on the electrode. Inspection of the electrode surface after multiple scans reveals the presence of an insoluble red film. During growth of the film, wave G decreases in intensity and eventually disappears, presumably due to the film blocking further monomer from reaching the electrode surface. This indicates that the film is insulating at 0.3 V vs SCE, since a conducting film would allow oxidation of monomer in solution at this potential even if the monomer is unable to penetrate to the electrode surface.

Bis(acetylide) **2c** shows four waves in its cyclic voltammogram, all of which appear relatively reversible (Figure 5a). The Ru(II/III) wave (K) appears very close to where it is observed for **2a** and **2b**. The three waves

(46) Martinez, F.; Voelkel, R.; Naegele, D.; Naarmann, H. *Mol. Cryst. Liq. Cryst.* **1989**, *167*, 227−232.

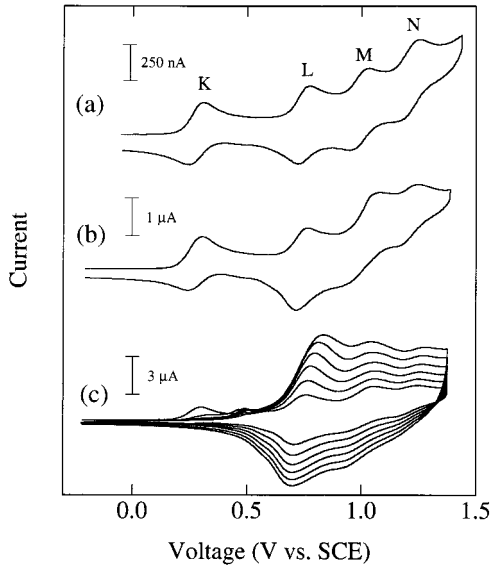

Figure 5. (a, b) Single-scan cyclic voltammograms of **2c** in CH_2Cl_2 containing 0.1 M $[(n\text{-}Bu)_4N]PF_6$: (a) 3.5×10^{-4} M; (b) 1.8×10^{-3} M. (c) Multiple-scan cyclic voltammogram of **2c** following the first scan (1.8×10^{-3} M). The scan rate was 100 mV/s.

(L−N) appearing at higher potential are ligand-based oxidations, by analogy with the results observed for **2a** and **2b**. When the concentration of the sample is increased, the shape of the voltammogram was found to change as a result of deposition of conducting material on the electrode during the scan (Figure 5b). Multiple scans show clear evidence for this growth (Figure 5c), analogous to the observations for **2b**. Extended scanning of solutions containing lower concentrations of **2c** (3.5×10^{-4} M, as in Figure 5a) also results in deposition of conducting material, albeit more slowly. Since the stability of the oxidized species formed under these conditions is in doubt, the exact nature of the conducting material formed in these experiments is unclear. It is possible that the material contains coordinated metal centers in addition to dimerized or polymerized oligothienyl ligands or, alternatively, that decomposition of the complexes via ligand loss results in polythiophene-like conducting polymer films. No films were formed when **1a**−**c** and **2a** were scanned repeatedly under the same conditions. Further investigations are needed to establish the exact nature of this material.

Vibrational and Electronic Spectra. The frequencies of the infrared absorption bands for the C≡C group in the complexes are collected in Table 2. The absorptions appear at similar energies for the whole series and are significantly lower in energy than the corresponding absorption for **4c**, demonstrating the extent of backbonding of the Ru(II) center to the acetylide.

The electronic spectra of **1a**−**c** are shown in Figure 6 and those of **2a**−**c** in Figure 7. All the complexes exhibit strong ligand-based (dppm) absorption bands between 230 and 270 nm. Intense absorption bands with λ_{max} in the range 328−460 nm are assigned to the thiophene-based $\pi-\pi^*$ transitions. These bands are absent in the spectra of analogous complexes which do not contain oligothienyl ligands, such as *trans*-$Ru(dppm)_2(Cl)(C{\equiv}CH)$,[47] and the extinction coefficients are in the range expected for such transitions.[48] These absorption

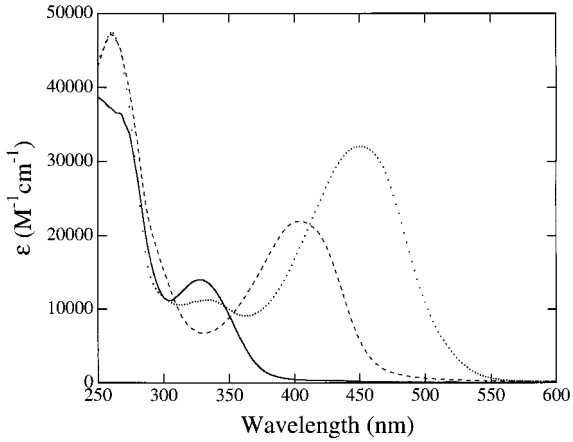

Figure 6. UV−visible spectra of **1a** (—), **1b** (- - -), and **1c** (···) in CH_2Cl_2.

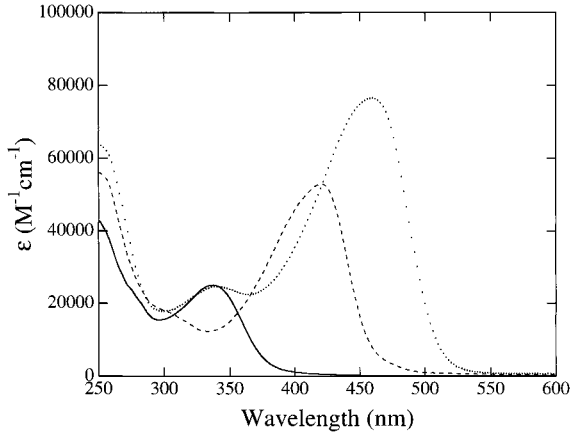

Figure 7. UV−visible spectra of **2a** (—), **2b** (- - -), and **2c** (···) in CH_2Cl_2.

bands are approximately twice as intense in the spectra of the bis(acetylides) **2a**−**c** as the corresponding bands for the mono(acetylides) **1a**−**c**, and the energy of the transition shifts to lower energy as the length of the oligothienyl ligand is increased. The energy of the $\pi-\pi^*$ absorption is 450 nm for **1c** and 460 nm for **2c**, while the absorption maximum for compound **4c** appears at 384 and 355 nm for 2,2′:5′,2″-terthiophene,[49] indicating that the electron-donating Ru(II) reduces the $\pi-\pi^*$ energy. The differences in λ_{max} are small between the mono(acetylide) and diacetylide containing the same ligand, from which we conclude that the $\pi-\pi^*$ transitions in the diacetylides are largely localized on each ligand rather than delocalized over the whole complex.

The instability of the Ru(III) complexes (vide supra) precluded us from obtaining electronic spectra of these species at room temperature; however, we were able to prepare solutions of the oxidized complexes by addition of 1 equiv of a freshly prepared solution of ferrocenium hexafluorophosphate to a solution of the neutral complex in dry CH_2Cl_2 at −20 °C. The solutions were transferred to a spectrophotometric cell held at −17 °C,

(47) This complex was prepared previously but was not characterized by cyclic voltammetry or UV−vis spectroscopy. See: Touchard, D.; Haquette, P.; Pirio, N.; Toupet, L.; Dixneuf, P. H. *Organometallics* **1993**, *12*, 3132−3139.

(48) Miller, L. L.; Yu, Y. *J. Org. Chem.* **1995**, *60*, 6813−6819.

(49) Pham, C. V.; Burkhardt, A.; Shabana, R.; Cunningham, D. D.; Mark, H. B.; Zimmer, H. *Phosphorus, Sulfur Silicon Relat. Elem.* **1989**, *46*, 153−168.

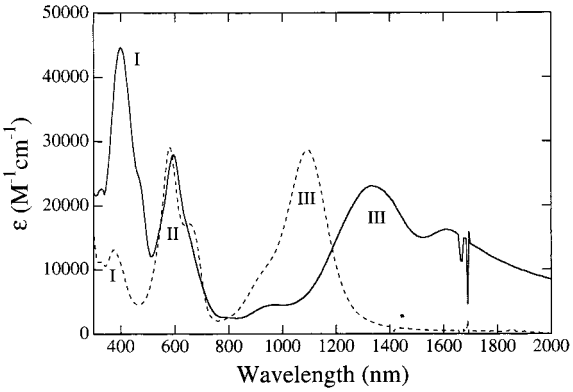

Figure 8. Visible−near-IR spectra of **1c**$^+$ (- - -) and **2c**$^+$ (—) in CH_2Cl_2 at −17 °C.

and the electronic spectra were obtained. The oxidation reactions were assumed to be complete when no further increase in the intensity of the new absorption bands was observed (within 30 min). After this time, the oxidized species **1c**$^+$ and **2c**$^+$ were stable in solution for at least 30 min with only very slight changes in their absorption spectra. Complexes **1a**$^+$, **1b**$^+$, **2a**$^+$, and **2b**$^+$ still decomposed at this temperature, as evidenced by changes in the color of the solutions, and we were unable to obtain reproducible spectra of these complexes. For these complexes oxidation and decomposition of the Ru(III) species occur at a comparable rate, resulting in mixtures of complexes in solution.

The electronic spectra of **1c**$^+$ and **2c**$^+$ at −17 °C are shown in Figure 8, and the data are summarized in Table 2. In these spectra, three sets of bands (I−III) are observed in the visible and near-IR regions. The ferrocenium used in the preparation is reduced to ferrocene, which has a d−d transition in this region; however, it is very weak (441 nm, $\epsilon = 91$ M^{-1} cm^{-1})[50] and does not interfere with the observed spectra. Band I is assigned to the $\pi-\pi^*$ absorption of the terthienyl group. This absorption is shifted to higher energy in the Ru(III) species, since the metal center is less electron-donating than in the corresponding Ru(II) complexes. Bands II and III consist of multiple, intense absorptions in the visible and near-IR region and are entirely absent in the spectra of the Ru(II) analogues. Ru(III) complexes frequently exhibit ligand-to-metal charge transfer (LMCT) absorptions,[51] particularly with reducing-type ligands. On the basis of the intensities and energies of bands II and III, we assign these as LMCT bands from the terthienyl ligand to Ru(III). Splitting of both ligand donor orbitals and metal acceptor orbitals would give rise to the multiple bands which are observed; however, it is not possible to assign these low-energy bands to specific transitions at this time.

Discussion

The electronic behavior of complexes **1a**−**c** and **2a**−**c** may be understood using the same theory which has been extensively applied to understanding the electronic behavior of mixed-valence bimetallic complexes.[52] The extent of electronic delocalization in such mixed-valence complexes has been probed using cyclic voltammetry and electronic spectroscopy and has been interpreted using a theory developed by Hush.[52] We consider the two redox-active centers (Ru and the oligothienyl group) in complexes **1a**−**c** and **2a**−**c** as analogous to the metal centers in heterobimetallic complexes.

In complexes **1a**−**c** and **2a**−**c** the length of the oligothienyl group has a dramatic effect on the oxidation potential of this group; however, it does not significantly affect the Ru(II/III) oxidation potential. This is similar to effects observed in bimetallic Fe(II) ferrocenylacetylide complexes by Sato.[53] These workers prepared (Cp or Cp*)(PP)FeC≡CFc complexes (PP = $Ph_2PCH_2CH_2PPh_2$ (dppe), $Ph_2PCH_2PPh_2$ (dppm), and $Me_2PCH_2PMe_2$ (dmpe); Fc = ferrocenyl) and showed that in these complexes the oxidation potential of the (Cp or Cp*)(PP)Fe− moiety varies from −0.47 to −0.84 V depending on the nature of the phosphine substituents, while the oxidation potential of the Fc group is relatively invariant (between +0.08 and +0.12 V). The strength of the intervalence charge transfer bands obtained for the mixed-valence derivatives of these complexes indicates that they are delocalized systems. It is apparent from these results that the extent of delocalization in heterobimetallic complexes is ascertained only from the *difference* in the redox potentials of the two metal centers. Likewise, the absolute Ru(II/III) redox potentials of **1a**−**c** and **2a**−**c** provide little direct insight into delocalization in these complexes.

Although the length of the oligothienyl ligand has little effect on the potential of the Ru(II/III) oxidation, the complexes containing the longer ligands were found to have more reversible Ru(II/III) oxidation waves. This is due to resonance delocalization of the positive charge in the Ru(III) species onto the oligothienyl group. This resonance stabilization is greater for more conjugated ligands and minimizes further chemical reactions of the oxidized complexes. This is consistent with the complete irreversibility of the Ru(II/III) wave in *trans*-$Ru(dppm)_2(Cl)(C{\equiv}CH)$,[47] in which no resonance stabilization is possible.

Delocalization of charge in the Ru(III) species should also result in low-energy, intense charge-transfer bands. Strong absorptions in the visible and near-IR regions are often observed in the spectra of mixed-valent bimetallic complexes due to intervalence charge transfer (IVCT).[51,52] The intensity of the absorption is related to the extent of delocalization of charge, and the energy of the transition has been correlated to the oxidation potential difference between the metals in heterobimetallic complexes.[38] The differences in the oxidation potentials of the terthienyl ligands and the Ru centers in **1c** and **2c** are 0.54 and 0.46 V, respectively, and the complex with the smaller difference in oxidation potentials between ligand and metal (**2c**) also has the lower energy LMCT band with the lowest energy absorptions observed at 1090 nm in **1c**$^+$ and at 1330 nm with a shoulder at 1610 nm in **2c**$^+$. Similarly, the difference in the oxidation potentials for the two Fe(II/III) couples

(50) Sohn, Y. S.; Hendrickson, D. N.; Gray, H. B. *J. Am. Chem. Soc.* **1971**, *93*, 3603.
(51) Lever, A. B. P. *Inorganic Electronic Spectroscopy*, 2nd ed.; Elsevier: New York, 1984.
(52) Hush, N. S. *Prog. Inorg. Chem.* **1967**, *8*, 391−444.
(53) Sato, M.; Hayashi, Y.; Kumakura, S.; Shinizu, N.; Katada, M.; Kawata, S. *Organometallics* **1996**, *15*, 721−728.

of Cp(dppe)FeC≡CFc (0.59 V) and Cp(dmpe)FeC≡CFc (0.80 V) correlates with the energy of the IVCT band.[53] The mixed-valence analogue of Cp(dppe)FeC≡CFc has an intense, broad IVCT band at 1590 nm, while Cp(dmpe)FeC≡CFc has a band at 1295 nm.

Conclusions

The results reported herein support the conclusion that the π system of the conjugated oligothienyl ligands interacts electronically with the Ru center. The electron-donating Ru(II) group decreases the energy of the $\pi-\pi^*$ transition in the oligothienyl ligands, and the energy of this transition increases when Ru(II) is oxidized to Ru(III). The reversibility of the Ru(II/III) oxidation wave improves as the length of the oligothienyl ligand is increased, indicating stabilization of the Ru(III) species occurs via delocalization of positive charge from the metal to the oligothienyl ligand. The presence of low-energy charge-transfer transitions in the spectra of **1c**$^+$ and **2c**$^+$ is consistent with this delocalization.

These results suggest that polymers containing Ru centers bridged by oligothienyl linkers could be conductive; however, it is clear that polymers incorporating these groups will require complete stability of the Ru center in both oxidation states, otherwise decomposition may result in the formation of material of ill-defined composition. This may be possible by tuning the oxidation potential of both the metal and the organic linker.

Experimental Section

General Considerations. All reactions were carried out under nitrogen using Schlenk techniques, unless noted otherwise. Diethyl ether and tetrahydrofuran were dried by refluxing over sodium/benzophenone. Diisopropylamine was purified by distillation from KOH and was stored over molecular sieves (4 Å). All other compounds were used as received. *trans*- and *cis*-Ru(dppm)$_2$Cl$_2$ (**3**),[54,55] Pd(PPh$_3$)$_2$Cl$_2$,[56] ferrocenium hexafluorophosphate (FcPF$_6$),[57] 1-(trimethylsilyl)-2-(2-thienyl)acetylene (**4a**),[58] (2-thienyl)acetylene (**5a**),[58] 2,2′-bithiophene,[58] 5-bromo-2,2′-bithiophene,[59] 2,2′:5′,2″-terthiophene,[60] and 5-iodo-2,2′:5′,2″-terthiophene[60] were all prepared using literature procedures. 1-(Trimethylsilyl)-2-(5-(2,2′-bithienyl))acetylene (**4b**) and (5-(2,2′-bithienyl))acetylene (**5b**) were prepared by modification of the procedures for the preparation of **4a** and **5a**, respectively.[58] 1-(Tributylstannyl)-2-(2-thienyl)acetylene (**7a**) and 1-(tributylstannyl)-2-(5-(2,2′-bithienyl))acetylene (**7b**) were prepared using the procedure for 1-(tributylstannyl)-2-(5-(2,2′:5′,2″-terthienyl))acetylene (**7c**) (vide infra) and used without further purification. ^{1}H, ^{13}C, and ^{31}P{^{1}H} NMR spectra were obtained on a Bruker CPX-200, Varian XL-300, or Bruker WH-400 spectrometer. Spectra were referenced to residual solvent (^{1}H, ^{13}C) or external 85% H_3PO_4 (^{31}P). Electrochemical measurements were conducted on a Pine AFCBP1 bipotentiostat using a Pt-disk working electrode, Pt-wire-coil counter electrode, and Ag -wire reference electrode. The supporting electrolyte was 0.1 M [(n-Bu)$_4$N]PF$_6$, and CH_2Cl_2 was used as the solvent. The concentration of the complexes was in the range (1.6−2.2) × 10^{-3} M unless otherwise noted. Decamethylferrocene (−0.12 V vs SCE) was used as an internal reference. Methylene chloride used in cyclic voltammetry was dried by refluxing over calcium hydride. The UV−visible spectra of **1a**−**c** and **2a**−**c** were obtained on a UNICAM spectrometer. The visible and near-IR spectra of **1a**−**c**$^+$ and **2a**−**c**$^+$ in dry CH_2Cl_2 solutions were collected on a Varian Cary 5 spectrometer, in which the sample cell was held at −17 °C under a nitrogen atmosphere.

1-(Trimethylsilyl)-2-(5-(2,2′:5′,2″-terthienyl))acetylene (4c). A suspension of 5-iodo-2,2′:5′,2″-terthiophene (0.64 g, 1.7 mmol), diisopropylamine (0.33 g, 3.3 mmol), Pd(PPh$_3$)$_2$Cl$_2$ (0.14 g, 0.20 mmol), and CuI (0.022 g, 0.12 mmol) in dry THF (60 mL) was degassed for 2 min with N_2. (Trimethylsilyl)-acetylene (0.33 g, 3.4 mmol) was added to the suspension via syringe. After it was stirred overnight at room temperature, the solution turned dark green. The reaction was quenched by adding distilled water (20 mL) to the solution. The organic layer was collected, and the aqueous layer was extracted with CH_2Cl_2 (2 × 20 mL). The organic extracts were combined and washed with brine (30 mL) and distilled water and then dried over anhydrous $MgSO_4$. The solvent was removed to give a brown solid, which was purified by flash chromatography (silica gel), using hexanes as eluant. Yield: 0.52 g (88%). ^{1}H NMR (400 MHz, $CDCl_3$): δ 7.21 (dd, J = 5.1, 1.0 Hz, 1H), 7.16 (dd, J = 3.6, 1.0 Hz, 1H), 7.12 (d, J = 3.8 Hz, 1H), 7.05 (s, 2H), 7.00 (dd, J = 5.1, 3.6 Hz, 1H), 6.97 (d, J = 3.8 Hz, 1H), 0.30 (s, 9H). ^{13}C{^{1}H} NMR (75.429 MHz, $CDCl_3$): δ 138.48, 136.85, 136.78, 135.22, 133.48, 127.86, 124.78, 124.66, 124.29, 123.84, 123.08, 121.72, 100.18, 97.39, −0.17. Anal. Calcd for $C_{17}H_{16}S_3Si$: C, 59.25; H, 4.68. Found: C, 59.18; H, 4.70.

5-(2,2′:5′,2″-Terthienyl)acetylene (5c). To a solution of **4c** (0.44 g, 1.3 mmol) in a mixture of $CHCl_3$ and MeOH (60 mL, 1:3 v/v) was added anhydrous K_2CO_3 (0.36 g, 2.6 mmol). The suspension was stirred at room temperature for 2 h, after which time the solvent was removed and the solid was extracted with $CHCl_3$ (20 mL). The $CHCl_3$ solution was then washed with distilled water (2 × 30 mL) and dried over anhydrous $MgSO_4$. The product was obtained as a yellow solid by removing the solvent and purified by flash chromatography (silica gel), using hexanes as eluant. Yield: 0.27 g (78%). ^{1}H NMR (400 MHz, $CDCl_3$): δ 7.22 (dd, J = 5.1, 1.1 Hz, 1H), 7.15−7.17 (m, 2H), 7.05−7.07 (m, 2H), 6.99−7.02 (m, 2H), 3.40 (s, 1H). ^{13}C{^{1}H} NMR (75.429 MHz, $CDCl_3$): δ 138.85, 137.06, 136.79, 135.09, 133.98, 127.93, 124.99, 124.79, 124.35, 123.96, 123.09, 120.56, 82.56, 82.38. Anal. Calcd for $C_{14}H_8S_3$: C, 61.73; H, 2.96. Found: C, 62.04; H 2.96.

(Diisopropylamino)tributylstannane. This compound was prepared by modification of a literature procedure.[61] n-BuLi (1.6 M in hexanes; 31.7 mL, 50.7 mmol) was diluted with dry diethyl ether (30 mL) and cooled to −78 °C. Diisopropylamine (5.19 g, 51.3 mmol) was cooled to −78 °C and added dropwise with stirring to the n-BuLi solution via cannula. Upon completion of the addition, the mixture was warmed to room temperature. A solution of tributyltin chloride (10.3 mL, 38.0 mmol) in dry diethyl ether (15 mL) was added to the stirred reaction mixture, causing an immediate color change to milky white. After it was heated to reflux for 4 h, the solution was stirred at room temperature for 12 h, after which time the mixture was a pale yellow cloudy suspension. The lithium chloride was removed by suction filtration through Celite under N_2. Removal of the solvent afforded an orange oil, which was distilled under vacuum to give a moisture-sensitive colorless oil (bp 152 °C at 0.15 mmHg). Yield: 9.01 g (61%). ^{1}H NMR (200.132 MHz, $CDCl_3$): δ 2.83 (septet, J =

(54) Chatt, J.; Shaw, B. L.; Field, A. E. *J. Chem. Soc.* **1964**, 3466−3475.
(55) Sullivan, B. P.; Meyer, T. J. *Inorg. Chem.* **1982**, *21*, 1037−1040.
(56) Itatani, H.; Bailar, J. C. *J. Am. Oil Chem. Soc.* **1967**, *44*, 147−151.
(57) Smart, J. C.; Pinsky, B. L. *J. Am. Chem. Soc.* **1980**, *102*, 1009−1015.
(58) Wu, R.; Schumm, J. S.; Pearson, D. L.; Tour, J. M. *J. Org. Chem.* **1996**, *61*, 6906−6921.
(59) Bäuerle, P.; Würthner, F.; Götz, G.; Effenberger, F. *Synthesis* **1993**, 1099−1103.
(60) MacEachern, A.; Soucy, C.; Leitch, L. C.; Arnason, J. T.; Morand, P. *Tetrahedron* **1988**, *44*, 2403−2412.
(61) Jones, K.; Lappert, M. F. *J. Chem. Soc.* **1965**, 1944−1951.

6.3 Hz, 2H), 1.51−1.64 (m, 6H), 1.16−1.39 (m, 12H), 0.97 (d, J = 6.3 Hz, 12 H), 0.86 (t, J = 7.3 Hz, 9H). Anal. Calcd for $C_{18}H_{41}NSn$: C, 55.40; H, 10.59; N, 3.59. Found: C, 55.38;, H, 10.68; N, 3.90.

1-(Tributylstannyl)-2-(5-(2,2′:5′,2″-terthienyl))acetylene (7c). This compound was prepared by modification of a published procedure.[62] (Diisopropylamino)tributylstannane (0.72 g, 1.8 mmol) was added to a flask charged with **5c** (0.50 g, 1.8 mmol). Dry THF (20 mL) was added to the mixture, and the solution was stirred overnight in the absence of light at room temperature. The THF was removed, and the residual oil was held in vacuo at room temperature overnight, affording a brown oil. Yield: 1.02 g (99%). ^{1}H NMR (400 MHz, $CDCl_3$): δ 7.20 (dd, J = 5.1, 1.0 Hz, 1H), 7.15 (dd, J = 3.6, 1.0 Hz, 1H), 7.06 (d, J = 3.8 Hz, 1H), 7.04 (s, 2H), 7.00 (dd, J = 5.1, 3.6 Hz, 1H), 6.97 (d, J = 3.8 Hz, 1H), 1.57−1.64 (m, 6H), 1.32−1.41 (m, 6H), 1.07 (t, J = 8.1 Hz, 6H), 0.93 (t, J = 7.3 Hz, 9H). Anal. Calcd for $C_{26}H_{34}S_3Sn$: C, 55.62; H, 6.10. Found: C, 55.84; H, 6.29.

***trans*-{Ru=C=CHR(dppm)$_2$(Cl)}[PF$_6$] (6a; R = 2-Thienyl).** To a solution of **3** (0.60 g, 0.64 mmol) and $NaPF_6$ (0.21 g, 1.3 mmol) in CH_2Cl_2 (75 mL) was added **5a** (0.15 g, 1.4 mmol). After it was stirred at room temperature for 18 h, the red-brown solution was filtered through a filter-paper-tipped cannula. The solvent was removed in vacuo and the residue rinsed with diethyl ether, affording a rust-colored solid, which was dried in vacuo at 90 °C for 6 days. Yield: 0.68 g (92%). ^{1}H NMR (400 MHz, $CDCl_3$): δ 7.15−7.45 (m, 40H), 6.87 (dd, J = 5.2, 0.9 Hz, 1H), 6.51 (dd, J = 5.2, 3.6 Hz, 1H), 5.30−5.40 (m, 2H), 5.01−5.10 (m, 3H), 3.22−3.25 (m, 1H). ^{31}P{^{1}H} NMR (81.015 MHz, $CDCl_3$): δ −18.1 (s). Anal. Calcd for $C_{56}H_{48}ClF_6P_5RuS$: C, 58.06; H, 4.18. Found: C, 57.70; H, 4.06.

***trans*-Ru(dppm)$_2$(Cl)(C≡CR) (1a; R = 2-Thienyl).** To a solution of **6a** (0.62 g, 0.54 mmol) in CH_2Cl_2 (40 mL) was added 1,8-diazabicyclo[5.4.0]undec-7-ene (DBU; 80 μL, 0.54 mmol) via syringe. The red-brown solution changed color quickly to yellow. After it was stirred at room temperature for 2 h, the reaction mixture was filtered through a filter-paper-tipped cannula, and the solvent was removed under vacuum. The resulting dark yellow solid was taken up in a minimum of THF and transferred via cannula to a Schlenk filter charged with neutral alumina (Brockman, activity I). The product was eluted with diethyl ether. Removal of the solvent at reduced pressure, followed by rinsing with hexanes, yielded a yellow solid, which was recrystallized from layered chloroform−hexanes. The crystals were crushed and dried in vacuo at 90 °C for 6 days. Yield: 0.36 g (66%). ^{1}H NMR (400 MHz, $CDCl_3$): δ 7.38−7.50 (m, 16H), 7.20−7.30 (m, 8H), 7.15 (t, J = 7.6 Hz, 8H), 7.09 (t, J = 7.6 Hz, 8H), 6.57−6.60 (m, 2H), 5.68 (dd, J = 2.6, 1.9 Hz, 1H), 4.88 (quintet, J = 4.2 Hz, 4H). ^{31}P{^{1}H} NMR (81.015 MHz, $CDCl_3$): δ −8.7 (s). Anal. Calcd for $C_{56}H_{47}ClP_4RuS$: C, 66.43; H, 4.68. Found: C, 66.33; H, 4.61.

***trans*-Ru(dppm)$_2$(Cl)(C≡CR) (1b; R = 5-(2,2′-Bithienyl)).** To a solution of **3** (0.31 g, 0.33 mmol) and $NaPF_6$ (0.16 g, 0.95 mmol) in CH_2Cl_2 (30 mL) was added **5b** (0.17 g, 0.89 mmol). The solution was stirred at room temperature for 7 h, resulting in a change of color to dark brown. The solution was then filtered through a filter-paper-tipped cannula, and a brown solid was obtained by removing the solvent. The solid was dissolved in CH_2Cl_2 and filtered through a short Al_2O_3 column (basic, Brockman activity I) to give an orange solution. The volume of the solution was reduced to approximately 1 mL and then added to hexanes (40 mL), yielding an orange-yellow solid. The solid was dried overnight in vacuo at room temperature. Yield: 0.16 g (44%). ^{1}H NMR (400 MHz, CD_2Cl_2): δ 7.50−7.56 (m, 8H), 7.41−7.47 (m, 8H), 7.34 (t, J = 7.4 Hz, 4H), 7.30 (t, J = 7.4 Hz, 4H), 7.22 (t, J = 7.6 Hz, 8H), 7.16 (t, J = 7.6 Hz, 8H), 7.10−7.12 (m, 1H), 6.96−6.98 (m, 2H), 6.70 (d, J = 3.4 Hz, 1H), 5.54 (d, J = 3.4 Hz, 1H), 4.86−4.99 (m, 4H). ^{31}P{^{1}H} NMR (81.015 MHz, $CDCl_3$): δ −8.9 (s). Anal. Calcd. for $C_{60}H_{49}ClP_4RuS_2$: C, 65.84; H, 4.51. Found: C, 65.92; H, 4.52.

***trans*-Ru(dppm)$_2$(Cl)(C≡CR) (1c; R = 5-(2,2′:5′,2″-Terthienyl)).** This compound was prepared as described for **1b**. Yield: 53%. ^{1}H NMR (400 MHz, CD_2Cl_2): δ 7.50−7.56 (m, 8H), 7.41−7.48 (m, 8H), 7.12−7.38 (m, 26H), 7.03−7.06 (m, 2H), 6.87 (broad, 1H), 6.72 (d, J = 3.7 Hz, 1H), 5.54 (broad, 1H), 4.86−4.98 (m, 4H). ^{31}P{^{1}H} NMR (81.015 MHz, $CDCl_3$): δ −8.9 (s). Anal. Calcd for $C_{64}H_{51}ClP_4RuS_3$: C, 65.33; H, 4.37. Found: C, 65.49; H, 4.42.

***trans*-Ru(dppm)$_2$(C≡CR)$_2$ (2a; R = 2-Thienyl).** To a deaerated solution of **3** (0.43 g, 0.46 mmol) and CuI (7 mg, 0.04 mmol) in chlorobenzene (25 mL), was added **7a** (0.73 g, 1.8 mmol). The solution was heated to reflux overnight and then cooled to room temperature. Chlorobenzene was removed, and the residual solid was dissolved in CH_2Cl_2. The CH_2Cl_2 solution was filtered through Celite to remove CuI. The filtrate was concentrated to approximately 10 mL and hexanes added. The solution was then cooled to −4 °C overnight, resulting in precipitation of **2a**. Yield: 0.30 g (60%) ^{1}H NMR (400 MHz, CD_2Cl_2): δ 7.47−7.55 (m, 16H), 7.28 (t, J = 7.4 Hz, 8H), 7.15 (t, J = 7.6 Hz, 16H), 6.63−6.66 (m, 4H), 5.87 (t, J = 2.3 Hz, 2H), 4.85 (quintet, J = 4.2 Hz, 4H). ^{31}P{^{1}H} NMR (81.015 MHz, CD_2Cl_2): δ −4.4 (s). Anal. Calcd for $C_{62}H_{50}P_4RuS_2$: C, 68.69; H, 4.65. Found: C, 68.43; H, 4.53.

***trans*-Ru(dppm)$_2$(C≡CR)$_2$ (2b; R = 5-(2,2′-Bithienyl)).** This compound was prepared as described for **2a**. Yield: 80%. ^{1}H NMR (400 MHz, $CDCl_3$): δ 7.42−7.48 (m, 16H), 7.26 (t, J = 7.4 Hz, 8H), 7.15 (t, J = 7.6 Hz, 16H), 7.07 (dd, J = 5.0, 1.2 Hz, 2H), 6.93−6.99 (m, 4H), 6.74 (d, J = 3.7 Hz, 2H), 5.69 (d, J = 3.7 Hz, 2H), 4.81 (quintet, J = 4.1 Hz, 4H). ^{31}P{^{1}H} NMR (81.015 MHz, $CDCl_3$): δ −6.3 (s). Anal. Calcd for $C_{70}H_{54}P_4RuS_4$: C, 67.35; H, 4.36. Found: C, 67.01; H, 4.47.

***trans*-Ru(dppm)$_2$(C≡CR)$_2$ (2c; R = 5-(2,2′:5′2″-Terthienyl)).** This compound was prepared as described for **2a**. Yield: 84%. ^{1}H NMR (400 MHz, $CDCl_3$): δ 7.41−7.47 (m, 16H), 7.27 (t, J = 7.4 Hz, 8H), 7.11−7.19 (m, 20H), 7.02 (d, J = 3.6 Hz, 2H), 7.00 (dd, J = 5.1, 3.6, 2H), 6.87 (d, J = 3.7 Hz, 2H), 6.75 (d, J = 3.7 Hz, 2H), 5.69 (d, J = 3.7 Hz, 2H), 4.82 (quintet, J = 4.0 Hz, 4H). ^{31}P{^{1}H} NMR (81.015 MHz, $CDCl_3$): δ −6.3 (s). Anal. Calcd for $C_{78}H_{58}P_4RuS_6$: C, 66.32; H, 4.14. Found: C, 65.98; H, 4.04.

X-ray Crystallography. Crystal Structure Determination. Crystal data for **2c**: $C_{78}H_{58}P_4RuS_6$, M_r = 1412.64, triclinic, space group $P\bar{1}$ (No. 2), a = 13.1663(9) Å, b = 15.5443(8) Å, c = 17.757(2) Å, α = 70.834(3)°, β = 83.6388(10)°, γ = 75.9874(6)°, V = 3328.7(4) Å^3, Z = 2, D(calcd) = 1.409 g cm^{-3}, μ(Mo Kα) = 5.65 cm^{-1}, F(000) = 1452. An orange irregular crystal of dimensions 0.40 × 0.35 × 0.20 mm was used.

Data Collection and Processing. Data were obtained on a Rigaku/ADSC CCD area detector with graphite-monochromated Mo Kα radiation (λ = 0.710 69 Å). The data were collected at a temperature of −93 °C. A total of 15 312 independent reflections were measured ($2\theta \leq 61°$), of which 8814 had $I > 3\sigma(I)$ and were considered to be observed. The data were corrected for Lorentz and polarization factors.

Structure Solution and Refinement. The structure was solved by direct methods and expanded using Fourier techniques. Both terminal thiophene moieties are disordered with respect to a 180° rotation about the bond to the adjacent ring. For the ring containing S(3) and the minor component S(3a), the disorder was modeled by split-atom refinement with bond length constraints. A similar treatment of the more nearly ordered ring containing S(6) was not successful. As a result of the disorder, both resolved and unresolved, the geometry of the terminal thiophene rings is subject to errors larger than expected from the least-squares standard deviations. All other

(62) Viola, E.; Lo Sterzo, C.; Crescenzi, R.; Frachey, G. *J. Organomet. Chem.* **1995**, *493*, C9−C13.

non-hydrogen atoms were refined anisotropically. Hydrogen atoms were fixed in idealized positions with C−H = 0.98 Å and thermal parameters 1.2 times those of the parent atoms. The final cycle of full-matrix least-squares refinement was based on the observed data and 809 variable parameters and converged with R1 = 0.037 and wR2 = 0.079. The maximum and minimum peaks on the final difference Fourier map corresponded to 1.92 and −1.28 e $Å^{-3}$, respectively. All calculations were performed using the teXsan crystallographic software package of Molecular Structure Corp.

Acknowledgment. We thank the Natural Sciences and Engineering Research Council of Canada for funding.

Supporting Information Available: Listings describing further details of the X-ray structural determination of **2c**. This material is available free of charge via the Internet at http://pubs.acs.org.

OM980677J